Beam cooler for low-energy radioactive ions

A. Nieminen[a],*, J. Huikari[a], A. Jokinen[a], J. Äystö[a,1], P. Campbell[b],
E.C.A. Cochrane[c,2]

[a]*Department of Physics, University of Jyväskylä, P.O. Box 35 (Y5), FIN-40351 Jyväskylä, Finland*
[b]*Department of Physics, Manchester University, Manchester M13 9PL, UK*
[c]*Department of Physics, University of Birmingham, Birmingham B15 2TT, UK*

EXOTRAPS collaboration

Abstract

An ion beam cooler for mass-separated radioactive ion beams has been developed and tested at the IGISOL-type mass separator facility. Technical description and characteristic properties are presented. An energy spread below 1 eV and transmission efficiency of 60% were measured. © 2001 Elsevier Science B.V. All rights reserved.

1. Introduction

At the IGISOL facility [1,2] radioactive ions for nuclear and collinear laser spectroscopy experiments are produced in nuclear reactions using ion beams from the Jyväskylä K-130 cyclotron. Reaction products thermalised as primary ions in helium are guided by a gas flow and by an electric field through a differentially pumped electrode system and accelerated to 40 keV energy for mass separation. This method is not limited by chemical

or physical properties of the element, and universally fast release of even refractory elements is possible. One drawback in the ion guide method is a relatively large energy spread (10–150 eV) [3] caused mainly by collisions with rest of the gas atoms during the extraction and acceleration process. A skimmer electrode with a small aperture of diam. 1.2 mm and a voltage V_{sk} with respect to the ion guide is used to "skim" away the helium gas and focus the ions through the aperture. The energy spread as well as the yield of radioactive ions increases with increasing skimmer voltage [3]. Sensitivity of the collinear laser spectroscopy at IGISOL is severely influenced by the beam quality and thus only by compromising the beam intensity the collinear laser spectroscopy has been feasible at IGISOL [4]. To improve the conditions for high-quality laser spectroscopy experiments the IGISOL

---

*Corresponding author. Tel.: + 358-14-260-2382.

E-mail address: arto.nieminen@phys.jyu.fi (A. Nieminen).

[1] Present address: EP-division, CERN, CH-1211 Geneva, Switzerland.

[2] Present address: Centre for Photobiology and Photodynamic Therapy, University of Leeds, Leeds LS2 9JT, UK.

ion beam quality has to be improved. Moreover, the chemical non-selectivity of the IGISOL method may result in considerable isobaric contaminations. This is especially true for fission and heavy ion induced reactions. Therefore, clean experiments on mass-separated beams of exotic nuclei at IGISOL require isobar purification which will be realised by employing the Penning trap injected by the external ion beam cooler. For maintaining the universality offered by the IGISOL technique the ion beam cooler introduced in this paper is a buffer-gas-filled RF quadrupole.

Collisional cooling of ions in three-dimensional radio frequency traps and in Penning traps is a well-understood field of study [5–7]. It was first proposed in two-dimensional RF quadrupole traps [8–10] by Douglas and French [11,12]. They noticed an increased ion transmission through a small aperture at the exit of linear RF quadrupole used as an interface between atmospheric pressure ion (API) source and a mass filter quadrupole when the RF quadrupole was operated at a relatively high pressure. Collisional focusing effects in an RF quadrupole for coupling an API source to a mass spectrometer quadrupole have also been studied theoretically by Tolmachev [13] and experimentally by Koslovsky et al. [14] who used air to cool Na$^+$, K$^+$ and Ce$^+$ ions. An RF quadrupole as a beam cooler was studied by Kim [15]. He proposed that such a beam cooler could be used at the ISOLTRAP facility [16] as a device for preparing a mass-separated 60 keV ion beam for injection into a Penning trap system. The cooling of mass-separated ion beams is also discussed in Ref. [17] in the context of reducing the beam emittance for mass measurements by MISTRAL [18] at ISOLDE/CERN.

2. Principle of the beam cooler

The IGISOL beam with an energy of 40 keV is decelerated to a suitable energy for injection into an RF quadrupole inside a buffer gas cell. The buffer gas cell is filled with helium at a pressure of the order of 0.1 mbar. While passing through helium and being confined in the RF quadrupole field ions lose their axial and transverse energy in collisions with the helium atoms and end up thermalised in

the axis of the quadrupole. Ions are essentially stopped in the axial direction and are left with a small-amplitude oscillation driven by the RF field. Their motion after being thermalised is governed by diffusion and space-charge effects. The thermalised ions then diffuse to the exit of the RF quadrupole where they are transported out of the gas cell and re-accelerated to an energy which is slightly lower than the incident energy due to a fraction lost in the collisional cooling. Since all the ions are thermalised and re-accelerated in high vacuum only the energy spread is removed.

For the transverse confinement of ions an RF quadrupole is used. The principle is the same as in quadrupole mass filter [9]. An RF voltage with amplitude V and angular frequency Ω is applied to the rods of a quadrupole in such a way that opposite rods are in the same RF phase and adjacent rods are in the opposite phase. In the mass filter there is also a DC component applied to the rods but in the RF quadrupole it is omitted to achieve optimum confinement of ions. The motion of ions in the RF quadrupole is governed by the so-called Mathieu parameter q [9]

$$q = \frac{4QV}{mr_0^2 \Omega^2} \tag{1}$$

which couples the particle parameters, charge Q and mass m to the quadrupole parameters, RF amplitude V, RF angular frequency Ω and size of the device r_0 which is defined as one half of the distance between the opposite rods. Ion motion is stable with $0 < q < 0.91$ [9]. The depth of the radial potential well [19,9] is given by

$$D = \frac{qV}{4}. \tag{2}$$

The so-called pseudopotential approximation is valid with low values of q (< 0.5) where the ion motion can be regarded as simple harmonic oscillation at macromotion frequency

$$\omega_0 = \frac{q}{2\sqrt{2}} \Omega. \tag{3}$$

The ions have additional oscillation, the so-called micromotion which comes from the driving RF field. The micromotion has the same frequency as the RF voltage Ω and amplitude proportional of

the electric field being zero in the axis and increasing linearly with the radius. At low values of q the micromotion is just a ripple on top of the macromotion but above $q = 0.5$ the micromotion amplitude is of the same order as the macromotion amplitude and it has to be taken into account. The optimal operating values for maximum transverse confinement are in the region of $q = 0.5$–0.6.

3. Technical design of the ion beam cooler

3.1. Electrostatic retardation

The beam cooler is located in the left beam line positioned at $30°$ angle with respect to the central beam line, see Fig. 1. The beam switchyard serving the left beam line is located at the focal plane of the separator. The incident ion beam is focused at the first deceleration electrode by the einzel lens placed half way between the cooler and the switchyard. The 40 keV IGISOL beam is decelerated before the injection by placing the cooler on a 40 kV high-voltage platform and focused in the gas cell through an entrance aperture by an electrostatic lens system, see Fig. 2. The final injection energy is

determined by the voltage of the high-voltage platform. Typical injection energy is about 100 eV. The lens system at entrance focuses the beam to a spot 4 mm in diameter with divergence $< 16°$ in order to match with the acceptance of the RFQ. The structure of the lens electrode system was designed by using the computer code SIMION [20].

3.2. RF quadrupole

The RF quadrupole consists of four cylindrical rods made out of stainless steel. The rods are divided into 16 segments separated from each other by a 0.5 mm gap, Fig. 2. The segments can be used electrically to produce an axial field. In this study the rod segments were wired together to form a single rod electrode. The overall length of the rods is 40 cm and the diameter is 2.3 cm. The shortest distance between the opposite pair of rods is $2r_0 = 2$ cm, where r_0 is the quadrupole dimension appearing in the Mathieu parameter q, see Section 2.

3.3. Extraction of ions

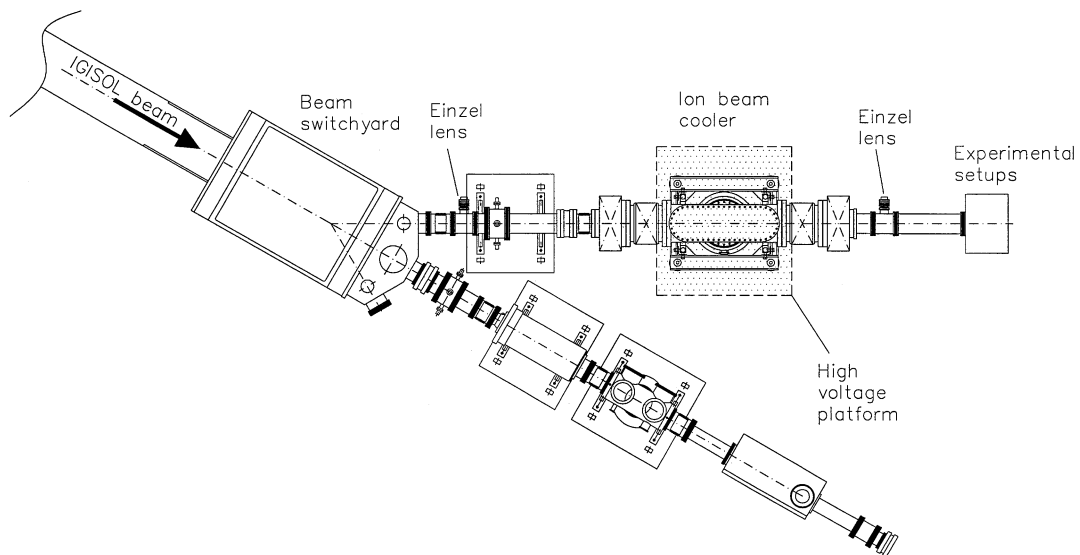Before acceleration, ions are transported out from the buffer gas cell to high vacuum, a miniature

Fig. 1. IGISOL beam lines. The left beam line is reserved for the ion beam cooler and the Penning trap which is currently under construction and not shown in this figure.
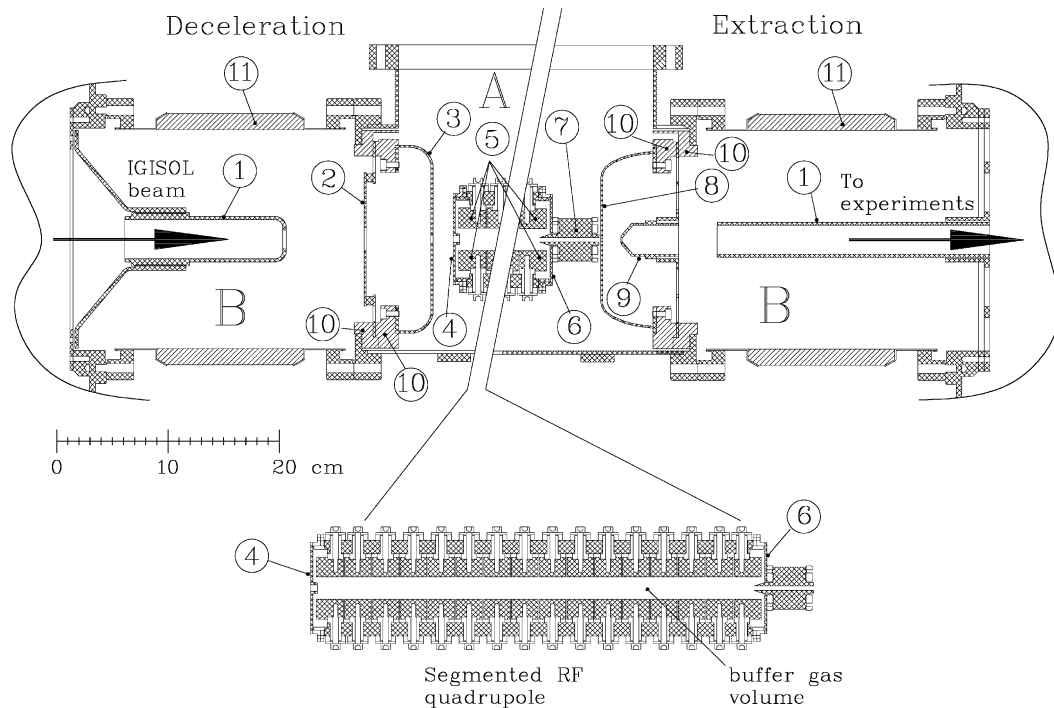
Fig. 2. The electrode configuration of the ion beam cooler. 1: ground electrode, 2: first deceleration electrode, 3: second deceleration electrode, 4: third deceleration electrode, 5: RF quadrupole rod segments, 6: end plate, 7: miniature quadrupole rods, 8: extraction plate, 9: extraction electrode, 10: isolator ring, 11: high-voltage isolator. The quadrupole rod segments are individually connected to a cylinder made out of stainless steel. The cylinder is closed by electrodes 4 and 6 to form the buffer gas volume. The gas is fed into the volume from the centre of the structure (not shown in this figure) and it is leaking out from the injection and extraction apertures to the volume A. The volume A is the first differential pumping stage separated from the second stage B by electrodes 3 and 8. The region between the high-voltage isolators is at 40 kV.

quadrupole concept proposed in Ref. [15] was adopted as a means to keep the ions confined in an RF field from the main quadrupole at ∼ 0.1 mbar to an intermediate vacuum section at 10^{-4} mbar. The miniature quadrupole dimension is $r'_0 = 1.5$ mm and it is 5 cm long of which 6 mm is inside the main quadrupole. The rods are made of stainless steel plates and are rounded for their inner edge and sharpened for their ends at the main quadrupole to minimise RF field distortion in the transition region, Fig. 2. The miniature quadrupole RF frequency and phases are the same as for the main quadrupole but the amplitude is a fraction of the main quadrupole amplitude. To have a smooth transition the amplitudes should behave as $V' = (r'^2_0/r^2_0)V$, where the primed symbols correspond to the miniature quadrupole. Typical

values are $V = 150$ V and $V' = 3.4$ V. The miniature quadrupole ends at the extraction plate which separates the first and second differential pumping stages. The DC level of the miniature quadrupole was set to 1 V below the main quadrupole level to ensure that the field distortion in the transition region will not prevent ions from entering the miniature quadrupole and exiting the cooler. An extraction electrode pulls the ions from the miniature quadrupole and after this ions are accelerated to their full energy again.

3.4. Differential pumping

The buffer gas volume is a cylinder closed at its ends by the third deceleration electrode and the end plate (+ miniature quadrupole). The open 0.91

volume of the cylinder is filled with ~ 0.1 mbar helium which is pumped through the entrance and exit apertures (areas 0.3 and 0.35 cm^2) by a 1600 l/s turbomolecular pump. The second differential pumping stage at injection is separated by the second deceleration electrode with a 6 mm aperture and at extraction by the extraction plate with a 2.7 mm aperture. The second stage is pumped by a 520 l/s turbomolecular pump at deceleration and by a 1000 l/s turbomolecular pump at the acceleration region, respectively. With this arrangement pressures of 10^{-4} and 10^{-6} mbar are achieved at first and second differential pumping stages, respectively with full buffer gas load.

4. Experimental studies

4.1. Influence of buffer gas pressure

In off-line tests the ion guide is replaced by a discharge ion source which produces ion beams from gaseous elements added in the helium or beams of solid elements from sputtering of the cathode material. The discharge ion source requires a glow discharge between the anode and cathode and hence only low pressures of less than 50 mbar can be used. This results in a smaller energy spread than that of an on-line produced ion beam. Off-line tests for studying the characteristics of the cooler were made by stable barium beams from a discharge ion source.

The buffer gas pressure is an important parameter in determining the transmission probability of ions through the cooler. First, the transmission was studied as a function of the cooler pressure. The RF parameters V and $f = \Omega/2\pi$ were chosen to have an optimum confinement and the focusing and deceleration lenses were tuned to have a maximum transmission at a fixed pressure. In first experiments the miniature quadrupole was not installed and ions were not extracted from the cooler. Instead the ion current to the end plate was measured. Similarly, the ion current through the 4 mm aperture in the end plate was measured by a Faraday cup at few volts lower potential behind it. The sum of these two currents equals the total current transmitted through the RFQ. Fig. 3 shows

these two currents and their sum as a function of pressure when the third deceleration electrode is at the same potential as the RFQ. At first the current transmitted through the end plate increases as the number of ions hitting the end plate decreases. The beam is cooled and reduced in size as the buffer gas pressure increases. At a certain point both currents start to decrease. This is because at higher pressure the range of the ions entering the buffer gas is shorter and consequently the ions lose their axial energy closer to the entrance. Therefore, it is more probable for an ion to diffuse back to the entrance than to go through the exit aperture. The same measurement was repeated with the third deceleration electrode set at 9.5 V above the RFQ potential. This created a potential barrier at the entrance preventing cooled ions from leaving the cooler in the wrong direction. As Fig. 3 shows, now the ion current going through the end plate increases with pressure and the current measured from the end plate decreases. After a certain pressure the current going through the end plate equals the total current. The total current at the end of RFQ remains constant with buffer gas pressure up to 0.3 mbar. Hence, there are no losses in the RFQ due to buffer gas collisions, in other words if an ion is captured at injection it is transported to the other end. After this the question of having optimum buffer gas pressure to cool the ion motion for transport through the exit aperture remains. Fig. 4 shows the same measurement repeated with ^{89}Y$^+$ beam employing the miniature quadrupole. The beam is also extracted and accelerated to 40 keV. Above a critical pressure p_C the transmission reaches the maximum and only a small loss with increasing pressure is observed. The critical pressure p_C depends on ion mass, axial field, incident energy spread and injection energy.

4.2. Influence of RF amplitude

According to the theory of RF quadrupoles [9] in Section 2, a certain combination of RF amplitude V and frequency f provides most efficient capture of ion with mass m in a quadrupole with radius r_0. The combination of amplitude and frequency for a given ion should result in $0 < q < 0.91$ to have ion motion mathematically stable. On the
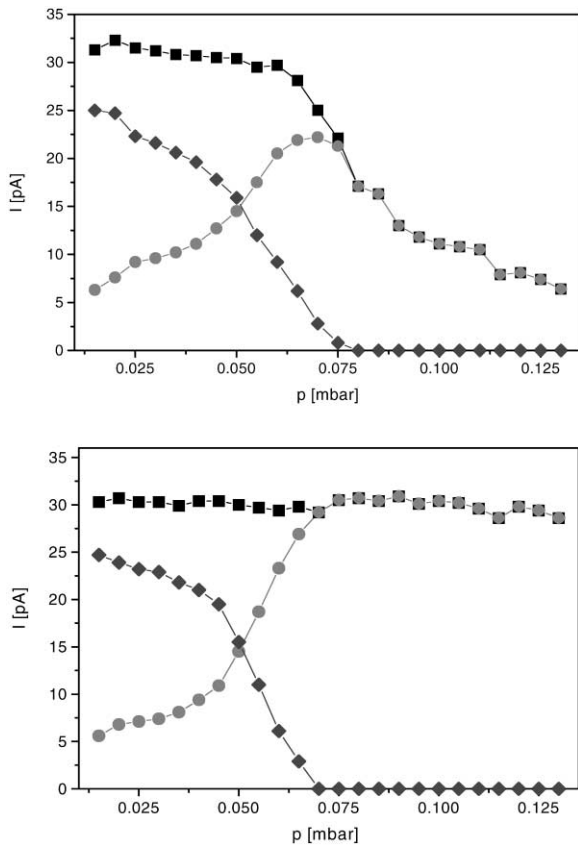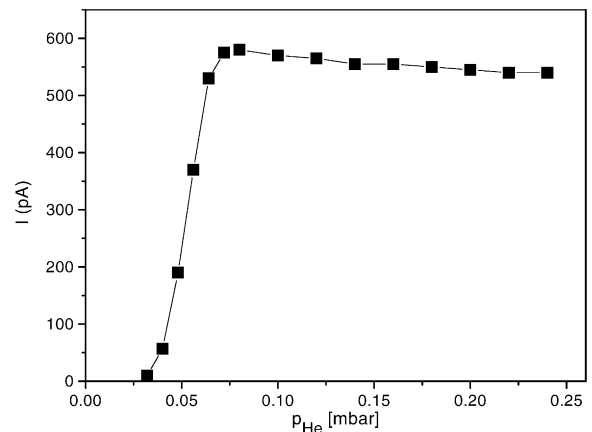
Fig. 4. Ion current transmitted through the cooler as a function of buffer gas pressure measured from a $^{89}Y^+$ beam extracted and accelerated to 40 keV. The curve shows that below a certain critical pressure ions suffer no collisions and thus their oscillation is not damped. Consequently, the characteristic oscillation amplitude is far too big for any ion to survive through the miniature quadrupole. As the pressure is increased, the number of ions that are radially cooled enough that they are captured and transported out of the cooler by the miniature quadrupole, is also increased. After the maximum is reached, increase of buffer gas pressure leads to no significant loss of ions.

Fig. 3. The ion beam current going through the quadrupole as a function of the buffer gas pressure. The current was measured from the end plate that had a 4 mm hole in the center (-◆-) and from a Faraday cup behind the end plate (-●-). The total current reaching the end of the quadrupole is then the sum of the mentioned currents (-■-). Top: The third deceleration electrode is at the same potential with the quadrupole. When buffer gas pressure is increased, the ions begin to leave the quadrupole from the injection side and the total current decreases. The current going through the end plate reaches zero as all the ions reaching the end of the structure are cooled and their oscillation amplitude is smaller than the end plate aperture radius. Bottom: The third deceleration electrode is at + 9.5 V above the quadrupole level creating a potential barrier at the entrance. The total current remains at constant value as the number of ions going through the end plate increases with increasing buffer gas pressure. At certain pressure all the ions are cooled to an oscillation amplitude smaller than the end plate aperture radius.

other hand, the depth of the pseudopotential well depends on the product qV. These together would imply that at a low value of q, although the ion motion is stable, the transmission is not good since

RFQ is not capable of capturing a diverging beam. At a higher value of q the transmission should increase since the pseudopotential well deepens. Close to the end of the stability diagram the micromotion amplitude gets larger and the beam, even though cooled is heated by the RF field and expands radially resulting in reduced transmission. At the edge of the stability diagram the transmission should go rapidly to zero.

The effect of RF parameters was tested off-line in the same geometry as in Section 4.1 by studying the ion current of $^{138}Ba^+$ on the end plate and Faraday cup behind it. Fig. 5 shows the transmitted currents as a function of Mathieu parameter q when buffer gas pressure was set to a value which was not enough to reduce the spatial size of the beam enough to fit through the end plate aperture. The value of q was changed by varying the RF amplitude keeping the RF frequency fixed at $f = 420$ kHz. The total transmitted ion current increases as a function of q and reaches maximum,

constant value at $q = 0.3$. At the edge of the stability region the transmitted ion current goes rapidly to zero as expected. The optimal region can be seen from the ion current measured from the end plate. Between $q = 0.4$ and 0.6 the current is at the minimum showing that at this region the radial confinement is optimal and the micromotion amplitude does not yet expand the spatial size of the beam. Near the edge this is the case as the ion current measured from the end plate has maximum at $q = 0.85$. The measurement was repeated on-line by radioactive $^{112}Rh^+$ ions produced in 29 MeV proton-induced fission of ^{238}U. The intensity of the mass-separated $^{112}Rh^+$ beam was 1×10^4 ions/s, and it was determined by measuring its strongest β-delayed γ transition of 349 keV. Fig. 5 shows the transmitted intensity as a function of RF amplitude with the fixed frequency of 550 kHz. The transmission is zero up to $q = 0.2$ which corresponds to the pseudopotential well depth of the miniature quadrupole of $D = 0.1$ eV. On the other hand, a 1 V drop in the DC potential at the entrance of the miniature quadrupole creates a radial potential hill with a maximum on the symmetry axis and to be able to capture the beam in the miniature quadrupole, the RFQ pseudopotential well has to compensate the effect of the radial DC potential hill. The transmission is at maximum and rather constant between $q = 0.5$ and 0.7. Near the edge of the stability region it decreases rapidly again as expected.

4.3. Energy spread

An important measure of the cooler's performance is the energy spread of the ion beam after cooling. The energy spread of the IGISOL beam is mainly introduced in the region between the exit nozzle of the ion guide and the skimmer where ions are accelerated in an electric field of 0.1–1 kV/cm under rather poor vacuum of 10^{-1} mbar. A part of the energy spread is also introduced at extraction where ions are accelerated with 10 kV in a vacuum of 10^{-4} mbar. The final energy spread depends on the ion guide pressure p_{IG} and skimmer voltage V_{sk}.

The first measurement of energy spread of cooled beam was done in an off-line test using $^{138}Ba^+$ ions and collinear laser spectroscopy. The beam was
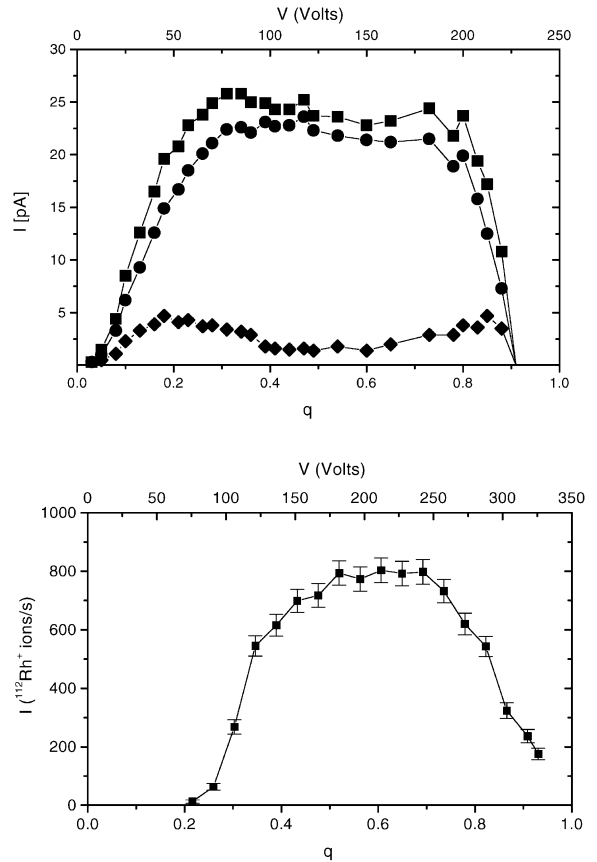

Fig. 5. Transmitted intensity as a function of the Mathieu parameter q which was varied by changing the RF amplitude while keeping the frequency fixed. Top: $^{138}Ba^+$ beam from a discharge ion source. Ion current measured from the end plate (-◆-), current through the end plate aperture (-●-) and the total current at the end of the quadrupole structure (-■-). The RF frequency was fixed at a value of 420 kHz. Bottom: Measured intensity of $^{112}Rh^+$ ions after the cooler as a function of RF amplitude. The intensity of the beam was deduced by measuring the strongest β-delayed γ transition of ^{112}Rh with $E_\gamma = 349$ keV. The RF frequency was fixed at 550 kHz.

sent through the cooler and reaccelerated to 40 keV. Narrow bandwidth laser beam was shined collinearly to the ion beam. The laser was locked to a frequency of 487.6178 THz and the energy of the ion beam was scanned in a resonance cell within few hundred eV to doppler shift the ions into resonance. Fluorescent light from excited ions was
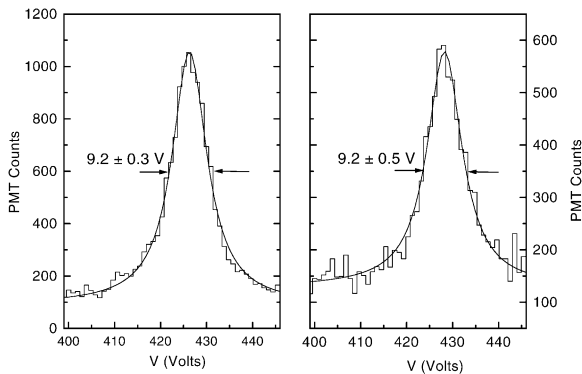
Fig. 6. Laser-induced resonances of cooled ^{138}Ba$^+$ ions produced by the discharge ion source. Left: Low incident beam energy spread can be obtained by applying only a low skimmer voltage of -12 V. The measured resonance serves as a reference with high-quality incident beam. Right: The incident beam energy spread is increased by applying a skimmer voltage of -250 V. Without cooling, the resonance would be broadened by the energy spread [21]. Here, no such effect is observed. Ion guide pressure in both is 22 mbar.

collected by an optical lens system and observed with a photomultiplier tube. The exact beam energy after the cooler was 36.992 keV, and an additional acceleration voltage of 430 V was needed to bring the ions into resonance, see Fig. 6. The measurement was repeated with low and high skimmer voltages, -12 V and -250 V, respectively, corresponding to an initial energy spreads of $\leqslant 10$ and $\leqslant 100$ eV [3]. In both cases the width of the resonance measured after the cooler was the same implying that the energy spread was reduced by the cooler. The measured overall widths at FWHM of the resonances with both skimmer voltages were 9.2 V. One should note that this is not the beam energy spread alone but the sum of the natural Lorenzian line width of the resonance and the Gaussian energy spread of the ion beam. The energy spread itself was extracted from the line shape by applying a fitting routine to separate the mentioned two components. From these measurements an upper limit of 4 eV can be given for the energy spread of the cooled Ba$^+$ beam.

Energy spread was also measured by different means in on-line conditions using ^{129}Xe$^+$ and ^{112}Rh$^+$ beams. Intense ion beams such as stable Xe$^+$ that are detectable by a Faraday cup, can be produced on-line by adding a trace amount of xenon which is then ionised by the primary cyclotron beam and energetic fission fragments. The energy spread was measured by applying a positive retarding voltage on the extraction plate and monitoring the transmitted beam intensity. The intensity does not change until a potential which exceeds the beam energy is reached at the extraction plate aperture. The intensity drops smoothly as the voltage on the extraction plate is increased. The energy spread is then obtained as a width of the differential of the intensity curve. The measurement was repeated for an intense (up to 5 nA) ^{129}Xe$^+$ beam monitoring the transmitted ion current as well as for normal on-line intensity beams ^{112}Rh$^+$ (1000 ions/s) monitoring transmitted activity, see Fig. 7. The energy spread in the former case was measured as 1.3 ± 0.1 eV and in the latter case 0.61 ± 0.09 eV.

4.4. Transmission measurements

When performing experiments on rare isotopes that are produced in minute amounts it is essential that the transmission efficiency of all ion optical elements is high. The overall transmission of the cooler was measured in an on-line experiment using β radioactive isotopes produced in proton-induced fission of ^{238}U. The radioactive beam with $A = 112$ was collected on a thin metal foil in front of a silicon surface barrier detector before and after the cooler. The corresponding yields were determined by the number of β decays observed. The cooler pressure was set high enough to get the best transmission for the highest skimmer voltage used, $V_{sk} = 300$ V corresponding to the widest energy spread of the ion guide. The measurement was repeated with different skimmer voltages. Fig. 8 shows the counting rate of the β detector before and after the cooler as a function of the skimmer voltage. The corresponding transmission efficiency of more than 60% was obtained with all the skimmer voltages used. Maximum transmission efficiency of about 70% is obtained at very low skimmer voltages corresponding to the lowest energy spread of the beam prior to the cooler.
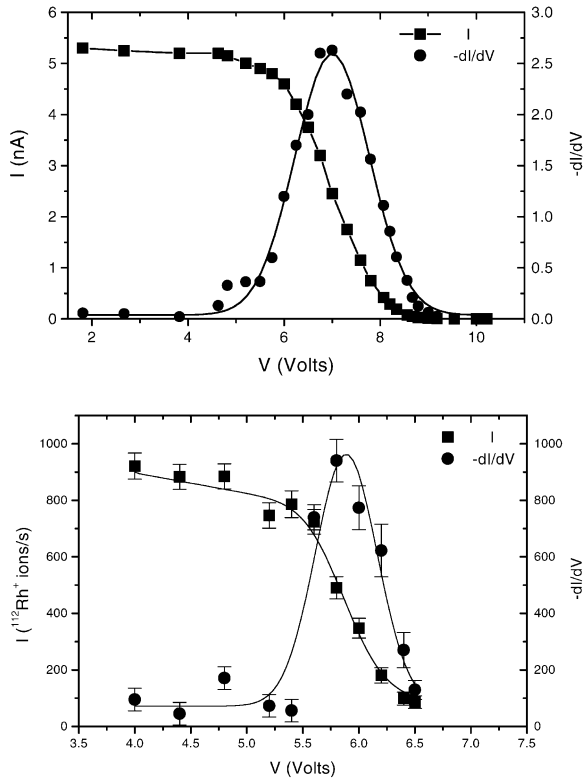
Fig. 7. Intensity of the ions that have transmitted through the cooler measured as a function of a blocking voltage. The beam energy profile is deduced by differentiating the intensity at the cut off. Top: Energy profile of the cooled beam when high-intensity stable beam of $^{128}Xe^+$ is used. The width of the profile is 1.3 ± 0.1 eV (FWHM). Bottom: Energy profile of the cooled beam measured using an on-line intensity beam of fission products with $A = 112$. The intensity was deduced from the 349 keV γ line. The width of the profile is 0.61 ± 0.09 eV.
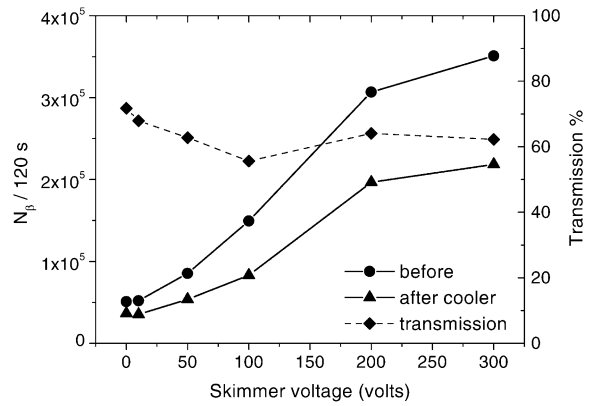

Fig. 8. The yield of radioactive isotopes with $A = 112$ measured as a function of skimmer voltage with two silicon detectors. The first one was located at the focal plane of the mass separator magnet before the cooler and the other one at the end of the beam line after the cooler. The yield follows the familiar trend with increasing skimmer voltage [3] both before and after the cooler. From the ratio of these a transmission efficiency of 60% can be deduced.

5. Discussion

It has been shown that a mass-separated ion beam can be cooled in an RF quadrupole cooler placed on a high-voltage platform. The resultant ion beam has ion optical properties that depend only on the cooler and not on the ion source. The 60% transmission still leaves some room for improvement but the final energy spread of the order of 1 eV is already in the regime aimed initially.

In all experiments performed in this work no mass analysis was done after the cooler. Therefore, there is no absolute information that all ions coming out have remained as singly charged atomic ions. However, in most cases studied radioactive ions were used to measure the transmitted intensity. The fact that ^{112}Rh could be identified by a well-known γ transition following β decay, is a manifestation that the beam coming out of the cooler is at least composed of what was put in. Also, the RF amplitude scans in Fig. 5 show the sharp decrease of transmitted ions at $q = 0.9$ implying that the masses of the ions are 138 and 112 amu, which were used in calculating the values of q. Kim reports on the widening of the stability region at high buffer gas pressures [15], but that effect was not observed at helium pressures used in the present work. The laser measurement proves also that Ba^+ ions survive as atomic ions since an ionic transition could be excited by laser and observed through fluorescent light from de-excitation.

The injection energy was a rather poorly known parameter in all measurements since the energy of the incoming beam was not exactly known. Usually the cooler high-voltage platform was set to a value where the transmission was at maximum. Then the difference between the acceleration voltage of

IGISOL and the cooler high voltage was of the order of 100–500 V. This difference is however not the final injection energy into the cooler due to the nozzle-skimmer region of the ion guide. The transmitted intensity through the cooler as a function of the cooler high voltage increases with HV to a maximum at an average injection energy of $\sim 100\,$V and then decreases sharply when the cooler high voltage becomes higher than the incoming beam energy. In the work of Kim [15] the transmission as a function of injection energy had a maximum of over 80% at 50 eV but had a rather smooth behaviour even up to 200 eV with the Mathieu q value around 0.6. At lower than 50 eV injection energies the transmission was sharply reduced. Considering the large energy spread in the IGISOL beam, the measured transmission efficiency is rather well in agreement with Ref. [15]. There is however no reason why the transmission should be much less than 100% since there were no losses observed due to addition of the buffer gas. Thus the transmission efficiency should be the same as the RF quadrupole capture efficiency and be governed by the matching of the incoming beam emittance and the RF quadrupole acceptance.

A measured energy spread of the ions exiting an RF quadrupole was reported in Refs. [14,15]. In Ref. [15], the reported energy spread of Cs^+ ions cooled by nitrogen buffer gas was about 0.1 eV. In Ref. [14], Na^+, K^+ and Cs^+ ions cooled with air resulted in 1 eV energy spread. The average final ion energies were 5 and 12.5 eV, respectively. The energy spread in this work is on the level of 1 eV. The final average energy is however nearly 40 keV and the values of few tenths of eV are already in the level of the high-voltage power supply stability.

Acknowledgements

References

[1] H. Penttilä et al., Nucl. Instr. and Meth. B 126 (1997) 213.

[2] P. Dendooven et al., Nucl. Instr. and Meth. B 126 (1997) 182.

[3] P. Taskinen, H. Penttilä, J. Äystö, P. Dendooven, P. Jauho, A. Jokinen, Nucl. Instr. and Meth. A 281 (1989) 539.

[4] J.L. Cooke et al., J. Phys. G 23 (1997) L97.

[5] F.G. Major, H.G. Dehmelt, Phys. Rev. 170 (1968) 91.

[6] R. Blatt et al., Z. Phys. D 4 (1986) 121.

[7] W.M. Itano, J.C. Bergquist, J.J. Bollinger, D.J. Wineland, Phys. Scripta T59 (1995) 106.

[8] W. Paul, H. Steinwedel, Z. Naturforsch. A8 (1953) 448.

[9] P. H. Dawson (Ed.), Quadrupole Mass Spectrometry and its Applications, Elsevier, Amsterdam, 1976.

[10] W. Paul, Rev. Mod. Phys. 62 (1990) 531.

[11] D.J. Douglas, J.B. French, J. Am. Soc. Mass Spectrom. 3 (1992) 398.

[12] D.J. Douglas, J. Am. Soc. Mass Spectrom. 9 (1998) 101.

[13] A.V. Tolmachev, I.V. Chernushevich, A.F. Dodonov, K.G. Standing, Nucl. Instr. and Meth. B 124 (1997) 112.

[14] V. Koslovsky et al., Int. J. Mass Spectrom. 181 (1998) 27.

[15] T. Kim, Ph.D. Thesis, McGill University, Montreal, 1997, unpublished.

[16] G. Bollen et al., Nucl. Instr. and Meth. A 368 (1996) 675.

[17] M.D. Lunney, R.B. Moore, Int. J. Mass Spectrom. 190/191 (1999) 153.

[18] M. de Saint-Simon et al., Phys. Scripta T59 (1995) 406.

[19] R.E. March, R.J. Hughes, Quadrupole Storage Mass Spectrometry, Wiley, New York, 1989.

[20] D.A. Dahl, J.E. Delmore, A.D. Appelhans, Rev. Sci. Instr. 61 (1990) 607.

[21] M. Huhta, Ph.D. Thesis, University of Jyväskylä, Jyväskylä, 1997, unpublished.